Proceedings of the ASME 2007 International Design Engineering Technical Conferences & Computers and Information in Engineering Conference
IDETC/CIE 2007
September 4-7, 2007, Las Vegas, Nevada, USA

DETC2007-35911

EXPERIMENTAL VALIDATION OF A COMPUTERIZED TOOL FOR FACE HOBBED GEAR CONTACT AND TENSILE STRESS ANALYSIS

Andrea Piazza
andrea.piazza@crf.it

Martino Vimercati

Powertrain Research and Technology – Centro Ricerche FIAT
Strada Torino 50 - 10043 Orbassano (TO), ITALY

ABSTRACT

While face milled gears have been widely analyzed, about face hobbed ones only very few studies have been developed and presented. Goal of this paper is to propose the validation of an accurate tool, which was presented by the authors in previous works, aimed to the computerized design of face hobbed gears. Firstly, the mathematical model able to compute detailed gear tooth surface representation on both spiral and hypoid gears will be briefly recalled; then, the so obtained 3D tooth geometry is employed as input for an advanced contact solver that, using a hybrid method combining finite element technique with semianalytical solutions, is able to efficiently carry out both contact analysis under light or heavy loads and stress tensile calculation. The validation analyses will be carried on published aerospace face hobbed spiral bevel gear data comparing measurements of root and fillet stresses. Good agreement with experimental results both in the time scale and in magnitude will be revealed.

1 INTRODUCTION

Spiral bevel and hypoid gear drives are widely applied in the transmission of many applications, such as helicopters, cars, trucks, etc. They are manufactured using mainly two cutting processes: face milling or face hobbing method. As well known, face milling process, traditionally adopted by the Gleason Works®, utilizes a circular face mill type cutter and employs an intermittent index. On the contrary, during FH process, traditionally adopted by Oerlikon® and in the last decades by the Gleason Works® as well, the work has continuous rotation and rotates in a timed relationship with the cutter: successive cutter blade groups engages successive tooth slots as the gear is being cut [1].

Many studies about tooth surface representation and design of FM spiral bevel and hypoid gears have been carried out [2-5]. On the contrary, about FH process, that is the considerably more complex, only a small number of works are available in the open literature [6-7].

The authors of this paper have worked extensively on that topic proposing a mathematical model aimed to the computation of the face hobbed gear tooth surfaces [8]; moreover they handled the output of this model in order to carry out a computerized design of these gears [9].

Goal of this paper is to provide the validation of that tool. To this end, a comparison with experimental data will be proposed; in particular the results collected by Handschuh et al. [10] will be considered. In that reference an experimental evaluation of the performance of an aerospace spiral bevel face-hobbed gear drive, in the following named TEST, is shown. In detail, results in terms of loaded tooth contact analysis, stress calculation and vibration/noise measurement are widely discussed. The basic characteristics of the TEST gear drive are summarized in Table 1.

Table 1. Basic characteristics of the TEST gear drive.

		Pinion	*Gear*
Module	[mm]	4.94	
Offset	[mm]	0	
Shaft Angle	[°]	90	
Teeth Number		12	36
Mean Spiral Angle	[°]	35.000	
Hand		LH	RH
Face Width	[mm]	25.4	
Mean Cone Distance	[mm]	81.05	
Nominal Pressure Angle	[°]	22.5	

The model validation requires the following steps. Starting from the information stored in Table 1, by means of a commercial gear design software, the geometric parameters, the basic machine settings and the cutting blade data will be firstly computed; after that, by means of the proposed model, the geometry of the tooth can be calculated and the gear drive performance under load can be evaluated. The main effort is devoted just to validate the model by comparing the stresses experimentally measured in the root and in the fillet area with the one numerically calculated; a qualitative comparison of the loaded tooth contact pattern will be also provided.

2 MODEL DESCRIPTION AND METHOD OF THE ANALYSIS

The first step in order to build a reliable numerical model is to get a fine geometrical representation of gear tooth surfaces. This is especially true when one is dealing with complex tooth geometry such as the face hobbing one. To this aim, a series of algorithms able to compute tooth surfaces of FH gears starting from cutting process has been implemented by the authors [8]. The geometry of real FH head cutter (Gleason Tri-Ac®) is considered; many kinds of blade configuration (straight and curve blades, with or without Toprem®) are taken into account. Then, according to the theory of gearing [11], FH cutting process (with and without generation motion) is simulated and gear tooth surfaces equations can be computed. The proposed mathematical model is able to provide an accurate description of the whole tooth, including fillet region; it also considers undercutting occurrence, which is very common in FH gears due to uniform depth tooth.

The obtained tooth surfaces are used as fundamental input for a powerful contact solver which is based on a semianalytical finite element formulation [12-13]. The gear drive can be study under light load by monitoring, for drive and coast side, the contact pattern and transmission error (i.e. it can be performed the commonly called Tooth Contact Analysis – TCA [14]). Moreover, with the aim to find out gear drive performance in the real service conditions, a set of torque values can be applied and the influence of the load on contact pattern, on transmission error and on load sharing can be accurately analyzed (Loaded Tooth Contact Analysis – LTCA [15]). Contact pressure and stress distribution can be also easily evaluated.

2. GEOMETRIC AND MANUFACTORING OF THE TEST GEAR DRIVE

Using the data collected in Table 1 as preliminary input for a commercial software for gear design (Gleason T2000®), a calculation aimed to reproduce the TEST gear drive has been attempted. Table 2 describes the obtained tooth geometry; Table 3 and 4 show the details regarding the machine setting and the cutting blades: the pinion is generated and the gear is Formate®; both the members are cut by means of curved blades using a head cutter with nominal radius equal to 76 mm and 13 blade groups.

Table 2. Tooth geometry data of the TEST gear drive.

		Pinion	*Gear*
Module	[mm]	4.941	
Offset	[mm]	0	
Shaft Angle	[°]	90	
Teeth Number		12	36
Mean Spiral Angle	[°]	35.000	35.000
Hand		LH	RH
Face Width	[mm]	25.4	25.4
Outer Cone Distance	[mm]	93.743	93.743
Pitch Angle	[°]	18.435	71.565
Addendum	[mm]	4.930	2.067
Dedendum	[mm]	2.942	5.805

Table 3. Basic machine settings for the TEST gear drive.

		Pinion		*Gear*	
		Concave	Convex	Concave	Convex
		Generated		Formate	
Radial Setting	[mm]	91.451	91.451	92.364	92.364
Tilt Angle	[°]	20.099	20.099	-	-
Swivel Angle	[°]	-25.371	-25.371	-	-
Blank Offset	[mm]	0.000	0.000	-	-
Machine Root Angle	[°]	0.154	0.154	71.565	71.565
Machine Center to Back	[mm]	-0.0722	-0.0722	-1.509	-1.509
Sliding Base	[mm]	13.865	13.865	-	-
Cradle Angle	[°]	53.697	49.817	51.405	51.405
Ratio of Roll	[mm]	2.999	2.999	-	-

Table 4. Cutting blades data for the TEST gear drive.

		Pinion		Gear	
		OB	IB	OB	IB
Blade Type		Curved	Curved	Curved	Curved
Blade Radius	[mm]	75.499	75.758	76.206	75.749
Blade Eccentric	[°]	17.832	17.633	17.738	17.846
Blade Height	[mm]	4.363	4.363	4.374	4.374
Blade Angle	[°]	25.323	18.122	22.231	21.681
Blade Groups Number		13	13	13	13
Nominal Rake Angle	[°]	12.000	12.000	12.000	12.000
Hook Angle	[°]	4.420	4.420	4.420	4.420
Cutter Edge Radius	[mm]	0.700	0.700	1.000	1.000
Blade Radius of Curvature	[mm]	762.000	762.000	762.000	762.000
Toprem Angle	[°]	-	-	-	-
Toprem Length	[mm]	-	-	-	-

3. TOOTH GEOMETRY OF THE TEST GEAR DRIVE

Figure 1 illustrates the tooth geometry representation obtained by means of the proposed model for the TEST gear drive.

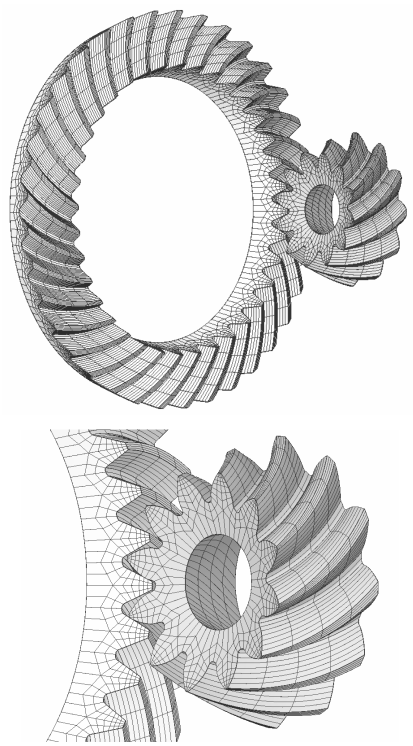

Figure 1. TEST gear tooth geometry representation.

Figure 2 describes the fillet area by means of the trend along the face width of the Nominal Root Line NRL, of the Real Root Line RRL and of the UnderCut/Fillet UC/FL line. According to that picture it is possible to note the tooth does not show undercut.

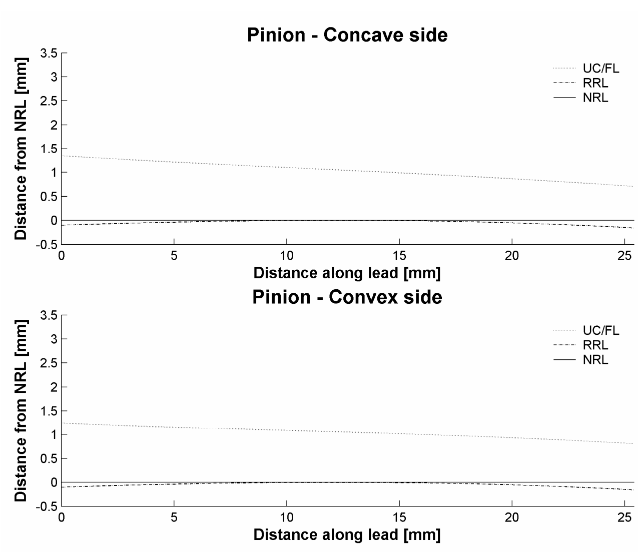

Figure 2. Details of the fillet area.

Due to the fact that the reference does not provide any topological data, just a qualitative comparison between the real tooth geometry and the one calculated by means of the numerical model is feasible (Figure 3).

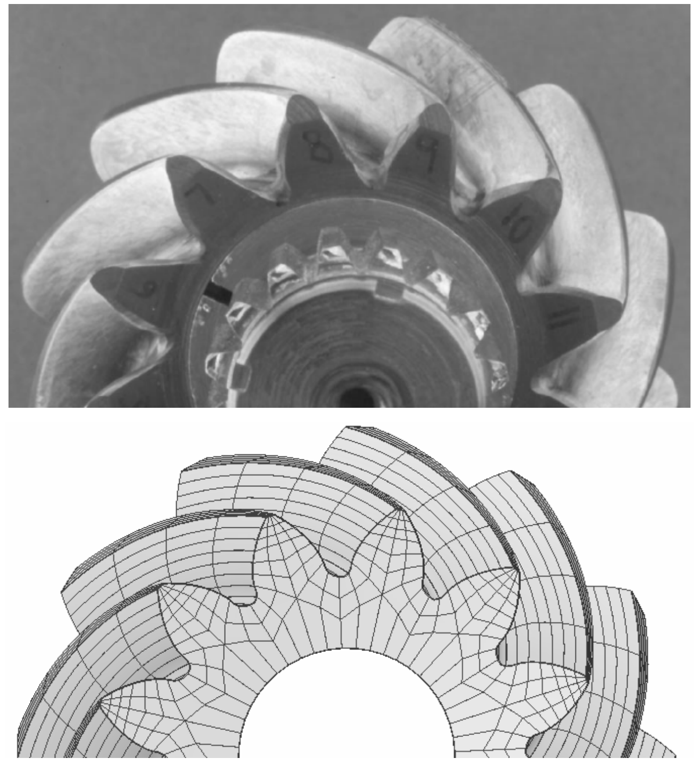

Figure 3. Qualitative comparison between the real pinion tooth geometry and the calculated one.

3.1 Evaluation of actual TEST gear fillet radius

Starting from the picture of the real pinion tooth (Figure 3 – above), a rough measurement of the radius of the fillet has been also attempted. Doing this way, referring to the toe of the concave side, a value about equal to 0.94 mm is obtained. When the same zone of the numerically computed tooth is considered, a value equal to 1.26 mm in correspondence of the maximum curvature point between the middle of inner surface and the contact surface is evaluated. The difference may be quite large (+34%) and, as it will be shown later, this evidence will have a significant influence on the fillet state of stress.

As known the fillet radius is strictly related to the edge radius of the cutting blade. The value used to cut the real tooth is unknown while in the numerical model it is assumed to be equal to 0.7 mm. In order to achieve a finer correspondence, models considering other edge radius values have been built. Namely, 0.5 mm and 0.3 mm have been tried obtaining the results summarized in Table 5 and Figure 4 (the points used for the radius calculation are highlighted). It can be noted that using an edge radius equal to 0.3 mm the best correspondence can be achieved.

Table 5. Comparison between the photo measured and the numerical fillet radius by varying edge radius.

Cutter Edge Radius [mm]	*Pinion Fillet Radius [mm]*	*Photo-measured Pinion Fillet Radius [mm]*	*Difference [%]*
0.70	1.26	~ 0.94	34.04
0.50	1.10	~ 0.94	17.02
0.30	0.98	~ 0.94	4.26

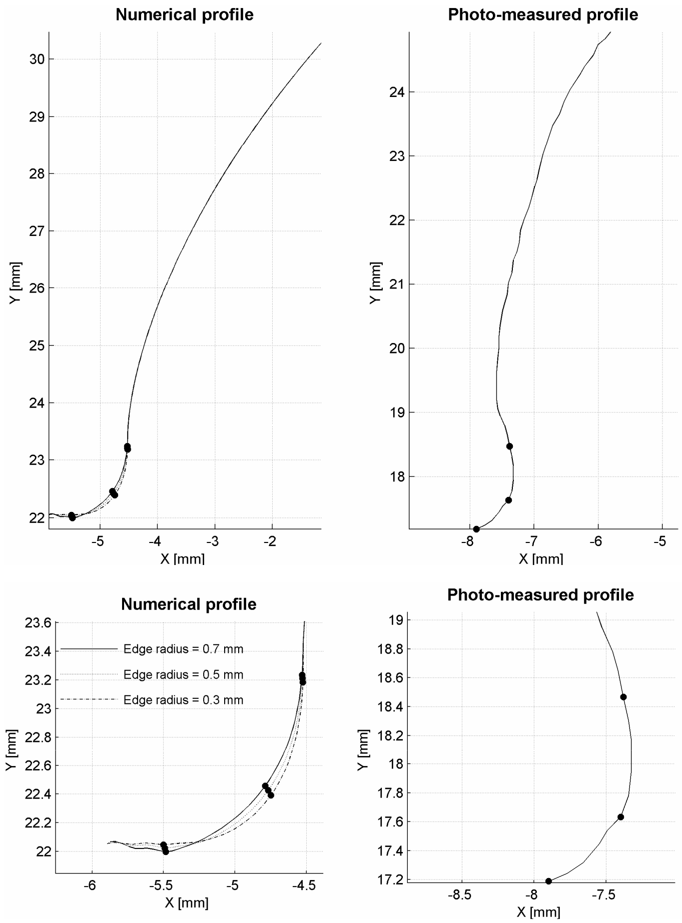

Figure 4. Comparison between the numerical pinion concave side profile and the photo-measured one (note that the reference systems are different).

4. STRESS CALCULATION

Referring to the experimental investigation, the stresses are evaluated by means of strain gages in the fillet area. In detail, referring to the sketch depicted in Figure 5, one strain gage at the heel position in the fillet and three strain gages (at heel, mid and toe positions) in the root (i.e. on the root cone).

On the other hand, with the aim to numerically compute the stresses, it is necessary to define a set of coordinates which are able to straightforwardly provide the stress measuring point on the tooth. Here, the curvilinear coordinate t which runs along the face width ($-1 \leq t \leq +1$ in Figure 6.a) and the curvilinear coordinate s which runs along the tooth profile ($0 \leq s \leq 48$ in Figure 6.b) have been defined. According to this schematization it is possible to affirm that the heel position corresponds to $t = +0.5$, the mid one to $t = 0$ and the toe one to $t = -0.5$; the root area is located in the range $0 \leq s \leq 2$ while the fillet one in the range $5 \leq s \leq 7$.

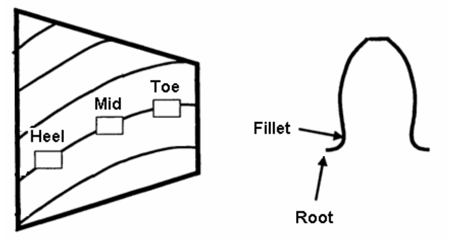

Figure 5. Sketch used in the TEST reference for location of the strain gages.

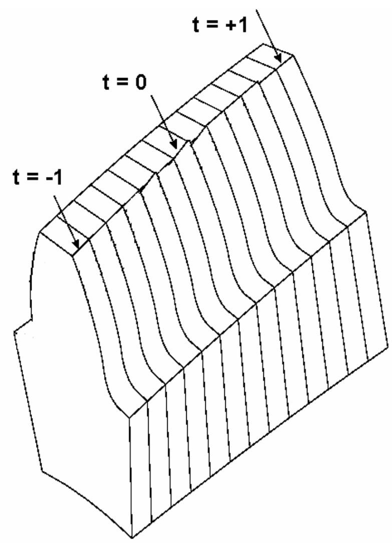

Figure 6.a. Schematization for defining the stress measuring section along the face width of the model.

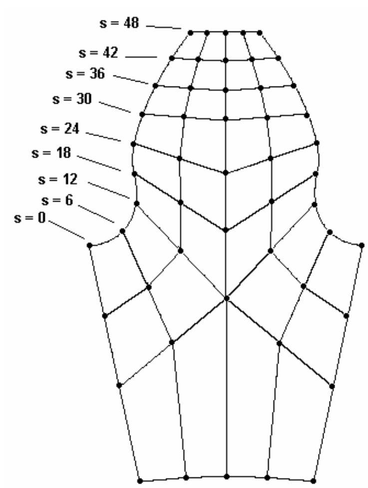

Figure 6.b. Schematization for defining the stress measuring point on a generic section of the model.

In Figure 7 the results of the TEST reference at a level of torque equal to 269 Nm are shown. In detail, the trend of bending stress vs time (during a whole meshing cycle) in the fillet and in the root region of the real pinion tooth is drawn. Referring to the same tooth position, Figure 8 reports the numerical results. According to the coordinates previously defined in Figure 6, the trend of the bending stress vs time in the fillet (s = 6) at the heel section (t = +0.5) and in the root (s = 1 o 2) in the mid, toe and heel section (t = 0, t = -0.5, t = +0.5) is shown.

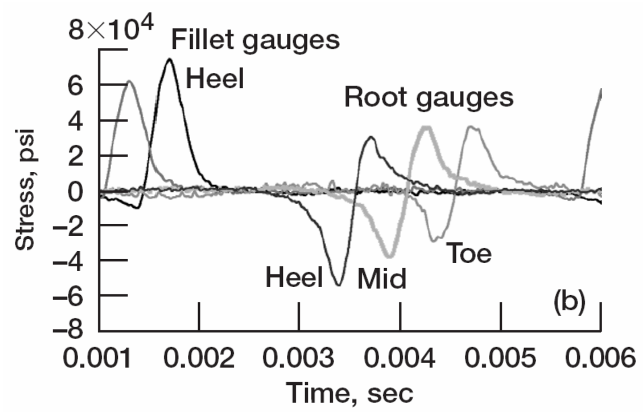

Figure 7. Pinion bending stress vs time as reported in the reference [10].

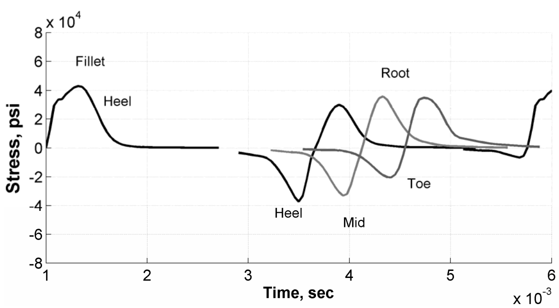

Figure 8. Pinion bending stress vs time as computed by the numerical model at an edge radius = 0.7 mm.

By analyzing these graphs and by considering Table 6 which summarizes the maximum/minimum stresses for each tooth position, it is possible to affirm that the differences between numerical results and the experimental one are quite small.

Table 6. Comparison between experimental and numerical analysis at 269 Nm.

	Fillet - Heel	
	Max	*Min*
TEST [MPa]	440.57	-39.30
Model [MPa]	296.35	-45.37
Difference %	32.73	-15.45

Root - Heel		*Root - Mid*		*Root - Toe*	
Max	*Min*	*Max*	*Min*	*Max*	*Min*
222.70	-384.73	258.55	-284.06	248.90	-221.32
206.87	-256.36	247.25	-227.79	240.11	-141.01
7.11	33.36	4.37	19.81	3.53	36.29

As stated in Table 7, similar evidences are collected at a lower level of torque (166 Nm).

Table 7. Experimental vs numerical stress results.

Edge radius = 0.7 mm @ 166 Nm

	Fillet - Heel	
	Max	*Min*
TEST [MPa]	278.55	-27.58
Model [MPa]	190.00	-35.00
Difference %	31.79	-26.91

Root - Heel		*Root - Mid*		*Root - Toe*	
Max	*Min*	*Max*	*Min*	*Max*	*Min*
139.96	-236.49	164.09	-239.25	166.85	-167.54
138.00	-287.00	176.37	-176.51	157.98	-104.71
1.40	-21.36	-7.48	26.22	5.32	37.50

It is reasonable to believe that the largest error value, which happens in the fillet-heel, is mainly due to two reasons. Firstly, it is quite difficult to find the exact correspondence between the experimental and the numerical stress measuring point; in fact, by studying Figure 9 which reports the numerical computed trend of the maximum principal stress in the fillet (s = 6) vs the position along the face width at 269 Nm, it is possible to note the value of the stress is significantly affected by the position along the face width.

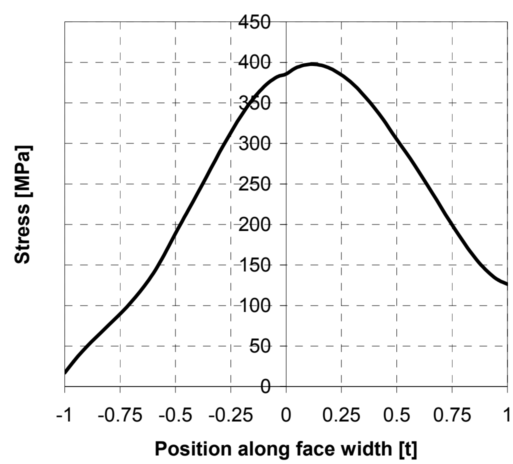

Figure 9. Numerically computed maximum principal stress vs position along face width in the fillet position.

Another issue to investigate is the influence of the value of the fillet radius on the bending stress. In fact, as previously detected, when a cutting blade edge radius value equal to 0.7 mm is used, the numerical pinion fillet radius (1.26 mm) is quite larger (+34%) than the real one (0.94 mm). In order to achieve a finer stress correspondence, models considering other edge radius values have been built. Namely, 0.5 mm and 0.3 mm have been tried obtaining the results summarized respectively in Table 8 and 9. Figure 10 summarizes the trend of the error between the maximum fillet-heel stress superimposed to the error between the fillet radius vs the cutting blade edge radius.

According to these results, it seems that for a value of cutting blade edge radius equal to 0.3 mm good agreement between numerical and experimental data is achieved.

Table 8. Experimental vs numerical stress analysis.
Edge radius = 0.5 mm @ 269 Nm

	Fillet - Heel		*Root - Heel*		*Root - Mid*		*Root - Toe*	
	Max	*Min*	*Max*	*Min*	*Max*	*Min*	*Max*	*Min*
TEST [MPa]	440.57	-39.30	222.70	-384.73	258.55	-284.06	248.90	-221.32
Model [MPa]	322.92	-58.95	176.49	-227.92	204.18	-221.57	213.33	-155.29
Difference %	26.70	-49.99	20.75	40.76	21.03	22.00	14.29	29.83

Table 9. Experimental vs numerical stress analysis.
Edge radius = 0.3 mm @ 269 Nm

	Fillet - Heel		*Root - Heel*		*Root - Mid*		*Root - Toe*	
	Max	*Min*	*Max*	*Min*	*Max*	*Min*	*Max*	*Min*
NASA [MPa]	440.57	-39.30	222.70	-384.73	258.55	-284.06	248.90	-221.32
Model [MPa]	351.98	-74.66	141.76	-196.90	159.53	-187.75	172.01	-134.15
Difference %	20.11	-89.98	36.34	48.82	38.30	33.91	30.89	39.39

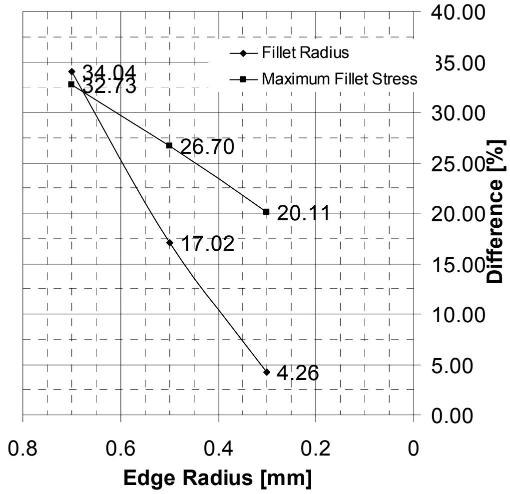

Figure 10. Differences between numerical and experimental results vs cutting edge radius at 269 Nm.

Similar behaviour is obtained at a level of torque equal to 166 Nm (Table 10 and 11 and Figure 11).

Table 10. Experimental vs numerical stress results.
Edge radius = 0.5 mm @ 166 Nm

	Fillet - Heel		*Root - Heel*		*Root - Mid*		*Root - Toe*	
	Max	*Min*	*Max*	*Min*	*Max*	*Min*	*Max*	*Min*
NASA [MPa]	278.55	-27.58	139.96	-236.49	164.09	-239.25	166.85	-167.54
Model [MPa]	201.27	-41.00	111.31	-159.91	142.98	-149.18	138.56	-96.00
Error %	27.74	-48.66	20.47	32.38	12.87	37.64	16.96	42.70

Table 11. Experimental vs numerical stress results.
Edge radius = 0.3 mm @ 166 Nm

	Fillet - Heel		*Root - Heel*		*Root - Mid*		*Root - Toe*	
	Max	*Min*	*Max*	*Min*	*Max*	*Min*	*Max*	*Min*
NASA [MPa]	278.55	-27.58	139.96	-236.49	164.09	-239.25	166.85	-167.54
Model [MPa]	219.51	-52.80	89.66	-138.22	111.69	-128.12	111.65	-83.01
Error %	21.19	-91.45	35.94	41.55	31.94	46.45	33.08	50.45

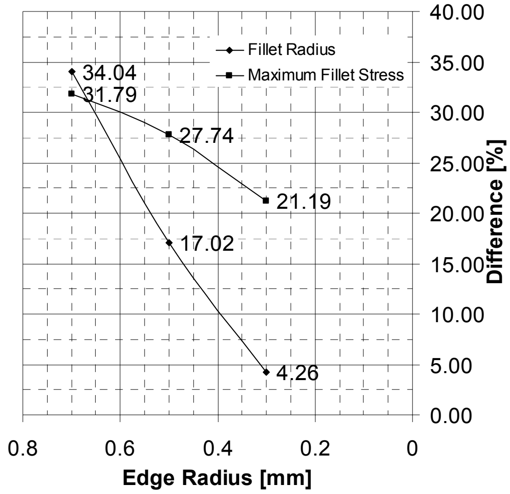

Figure 11. Difference between numerical and experimental results vs cutting edge radius at 166 Nm.

5. LOADED TOOTH CONTACT ANALYSIS

Figure 12 shows the tooth contact pattern which was experimentally measured at a level of torque equal to 269 Nm compared with the one numerically computed by means of the model. In both of the cases the pattern enlarges nearly on the whole face width assuming a similar shape.

Figure 12. Comparison of the experimental loaded tooth contact pattern (above) with the numerical one (below).

6 CONCLUSIONS

In this paper the validation of a tool previously developed by the author for computerized design of face hobbed hypoid gears has been proposed.

A reference case has been firstly chosen: experimental data collected on an aerospace spiral bevel face-hobbed gear drive by Handschuh et al. has been considered.

Then, by means of the proposed model, the geometry of the tooth has been calculated. Focusing the attention on the fillet radius, a comparison between the real tooth geometry and the numerical one has been attempted finding an acceptable correspondence, even if the result are strictly related to the value of the edge radius of the cutting blade (in the best case differences are lower than 5 %).

Next, the stresses experimentally measured in the root and in the fillet area with the one numerically calculated have been compared. While a satisfactory agreement has been achieved in the root area (both in the time scale and in magnitude), in the tooth fillet some discrepancies has been revealed and some additional consideration has to be done. Firstly, it is not so straightforwardly to catch the exact correspondence between the experimental and the numerical stress measuring point; this is a significant consideration being the value of the stress notably affected by the position along the face width. Another issue to point out is the influence of the value of the fillet radius on the bending stress. In fact, as previously mentioned, differences in the numerical fillet radius vs the real have been detected.

Finally, loaded tooth contact pattern has been also compared finding a reasonable agreement.

All these considerations allow to conclude that the model can be considered a reliable numerical tool for studying face hobbed hypoid gear drive.

ACKNOWLEDGMENTS

The authors would like to sincerely thank Robert F. Handschuh of the U.S. Army Research Laboratory, Glenn Research Center, Cleveland, Ohio for his kind support.

REFERENCES

[1] Stadtfeld, H.J., 2000, *Advanced Bevel Gear Technology*, The Gleason Works, Rochester, New York.

[2] Litvin, F.L. and Gutman, Y., 1981, "Methods of Synthesis and Analysis for Hypoid Gear-Drives of ''Formate'' and ''Helixform'', Part 1, 2, and 3", *ASME Journal of Mechanical Design*, Vol. **103 (1)**, pp. 83-113.

[3] Argyris J., Fuentes A. and Litvin F. L., 2002, "Computerized Integrated Approach for Design and Stress Analysis of Spiral Bevel Gears", *Computer Methods in Applied Mechanics and Engineering*, Vol. **191**, pp. 1057-1095.

[4] Gosselin, C., Guertin, T., Remond, D. and Jean, Y., 2000, "Simulation and Experimental Measurement of the Transmission Error of Real Hypoid Gears Under Load",

ASME Journa of. Mechanical Design, Vol. **122**, pp. 109-122.

[5] Lin, C.Y., Tsay, C.B. and Fong, Z.H. 1997, "Mathematical Model of Spiral Bevel and Hypoid Gears Manufactured by the Modified Roll Method", *Mechanism and Machine Theory*, Vol. **32 (2)**, pp. 121-136

[6] Fan, Q., Dafoe, R. S. and Swanger Jr., J, 2005, "Development of bevel gear face hobbing simulation and software", *International Conference on Gears*, Munich, Germany, (September 2005).

[7] Yi-Pei Shih, Zhang-Hua Fong, and Grandle C. Y. Lin, 2007, "Mathematical Model for a Universal Face Hobbing Hypoid Gear Generator", *Journal of Mechanical Design*, Vol. **129**, pp.38-47.

[8] Vimercati, M., 2006, "Mathematical Model for Tooth Surfaces Representation of Face-Hobbed Hypoid Gears and its Application to Contact Analysis and Stress Calculation", in press on *Mechanism and Machine Theory*, available on line August 2006.

[9] Vimercati, M. and Piazza, A., 2005, "Computerized Design of Face Hobbed Hypoid Gears: Tooth Surfaces Generation, Contact Analysis and Stress Calculation", *AGMA Fall Technical Meeting 2005*, Detroit, Michigan, (October 2005).

[10] Handschuh, R. F., Nanlawala, M., Hawkins, J. M. and Mahan D., 2001, "Experimental Comparison of Face-Milled and Face-Hobbed Spiral Bevel Gears", *NASA/TM-2001-210940, ARL-TR-1104*.

[11] Litvin, F.L., 1994, *Gear Geometry and Applied Theory*, Prentice Hall, Englewood Cliffs, New Jersey.

[12] Vijayakar, S.M., 2003, *Calyx Users Manual*, Advanced Numerical Solution, Hilliard, Ohio.

[13] Vijayakar, S.M., 1991, "A Combined Surface Integral and Finite Element Solution for a Three-Dimensional Contact Problem", *International Journal of Numerical Methods Engineering*, Vol. **31**, pp. 525–545.

[14] *Understanding Tooth Contact Analysis*, Gleason Works Publication, SD3139, 1978

[15] Krenzer, T.J., 1981, *Tooth Contact Analysis of Spiral Bevel and Hypoid Gears Under Load*, The Gleason Works, Rochester, New York.